IEEE P802.15
Wireless Personal Area Networks

Project	IEEE P802.15 Working Group for Wireless Personal Area Networks (WPANs)
Title	**The Ultra-wideband Indoor Path Loss Model**
Date Submitted	June 24, 2002
Source	Dr. Saeed S. Ghassemzadeh AT&T Labs-Research Rm. B237, 180 Park Ave. Florham park, NJ 07932 Voice: 973-236-6793 Fax: 973-360-5877 E-mail: saeedg@research.att.com Prof. Vahid Tarokh Division of Engineering & Applied Sciences Harvard University 33 Oxford Street Room MD 131 Cambridge, MA 02138 Voice: 617-384-5026 Fax: 617-496-6404 E-mail: vahid@deas.harvard.edu
Re:	[IEEE P802.15-02/208r1-SG3a]
Abstract	This contribution describes a simple statistical model for evaluating the path loss in indoor environments. It consists of detailed characterization of path loss model parameters of Ultra-Wideband (UWB) signals having a nominal center frequency of 5 GHz. The proposed statistical path loss model is for in-home UWB channel and it is based on over 300,000 frequency response measurements.
Purpose	For IEEE 802.15.SG3a to adopt the path loss model and use it in link budget calculations for validation of throughput and range requirements of UWB PHY proposals.
Notice	
Release	

Introduction

Many indoor propagation path loss models are available in the literature for path loss predictions and simulation of indoor UWB channel (See [3]-[15]). Regression analysis of our extensive UWB indoor experiments has led us to a unique one-slope statistical characterization [16] of the decibel-path loss as a function of decibel-distance for the indoor UWB channel. Our path loss model is unique in a sense that its two major parameters of its characterization mainly, path loss exponent and shadow fading standard deviation (in dB) are treated as normal random variables that change from one home to another or location to location. We will demonstrate that not only this statistical model follows the variation of the path loss in various homes; it can be upgraded as more data becomes available in the future.

In Section 1, we describe the data collection method and procedures. Section 2 gives details of data reduction. In Section 3 we represent our model followed by summary and references.

1. Measurements: Background, Equipment, Experiment Procedure

1.1. Background

Because of the Fourier transform relationship between the channel impulse response and the channel transfer function in the frequency domain, it is possible to measure the channel impulse response using the frequency domain (See [1] and [2]). This technique has been proven as accurate as many time domain techniques when real-time and long-distance measurements are not required (See [9]-[11]).

1.2. Equipment

Figure 1 illustrates the transceiver configurations. A Vector Network Analyzer (VNA) is used for measuring the frequency response of the channel. The VNA generates a signal as the input to a variable attenuator and a 34 dB gain broadband transmitter RF amplifier chain. The output of the RF power amplifier is propagated by a vertically polarized, conical monopole, omni-directional (in the H-plane) over the 4.375 – 5.625 GHz frequency range. The signal from the identical conical monopole receive antenna is first passed through a Low Noise Amplifier (LNA) with a gain of 34 dB. It is then returned to the VNA via 150 feet of coaxial cable with a 17-dB loss followed by another LNA with a gain of 36 dB. High quality doubly shielded cable was used to insure no leakage from the air into the receiver by the cable. The VNA records the variation of 401 complex tones across the above-mentioned frequency range. The VNA sweeps the frequency range for 401 received tones and compares them to pre-calibrated coefficients. The sweep rate for all tones is slightly over 400 ms corresponding to a maximum measurable Doppler spread of about 2.5 Hz. Programs in HP VEE software were written to control the VNA measurement system. The complex data from the VNA was stored on a laptop computer via a GP-IB interface.

1.3. Experiment Procedures

Using the techniques and hardware mentioned above, experiments were performed inside 23 homes in the northern and central New Jersey area. The homes had differing structure, age, size and clutter. The transmit antenna from the VNA was always located in a fixed position, and the dual receiving antenna mast was moved throughout the houses on a pre-measured grid. Knowledge of the physical distance between the transmitter and the receiver allowed the measured data to be correlated with the distance. For all measurements, the height of the transmit/receive antennas was fixed at 1.8 m (6-feet). Figure 2 illustrates typical home layout and measurement setup.

Measurements were made while the transmit/receive antennas were within Line-of-Sight (LOS) of each other or while they were within non-LOS (NLOS) of each other. Two different experiments were performed in each home. In 15 homes, we selected over 20 LOS locations and over 20 NLOS locations. We then measured the channel frequency response observed from two antennas separated by 38 inches, simultaneously, over a 1.8-minute period (273 snapshots). In the remaining 8 homes, we used only one receive antenna, 10 LOS, and 10 NLOS locations. Hence, our database contains about 1240×273 measurements of the channel frequency response. The transmit antenna location was placed for best signal coverage inside each home and optimized for minimum possible T-R separation for NLOS experiments. The transmitter's power level was adjusted so that the VNA always operated within the linear range of its detectors and well above noise floor. All measurements were performed on the same floor of each home so that variations in the pattern of the receiving and transmitting antenna did not have to be taken into account.

2. Data Reduction: Background, Scatter plots and Key Findings

2.1. Background

Within this contribution we refer to mean path loss as the transmit power multiplied by transmit and receive antenna gains divided by mean received power. That is:

$$PL = \frac{P_t \cdot G_t \cdot G_r}{\overline{P_r}} \qquad (1)$$

In our study, we measure the local mean path loss by time and frequency averaging of a swept CW transmission over the UWB bandwidth (e.g. 1.25 GHz) by a fixed receiver. Using the measured complex frequency response data, $H(f_i, t_j; d)$, we estimate the local mean path loss at any distance, d, by performing the following on :

$$Pl(d) = \frac{1}{MN}\sum_{i=1}^{N}\sum_{j=1}^{M}\left|H(f_i, t_j; d)\right|^2 \quad (2)$$

where N is the number of observed frequencies and M is the number of frequency response snap shots over time at d meters.

It is well known that the median of this path loss is directly proportional to d raised to some exponent γ (See [6],[8],[9],[13] and [14]). The path loss in dB at some distance d is then:

$$PL(d) = PL_0 + 10 \cdot \gamma \log_{10}\left(\frac{d}{d_0}\right) + S(d);\ d \geq d_0 = 1 \text{ m} \quad (3)$$

where PL_0 , the intercept point, is the path loss (i.e., Pl_0 in dB) at d=1 m, $10\gamma \cdot \log_{10}(d/d_0)$ is the median path loss referenced to 1 m; γ is referred to as the path loss exponent which depends on the structure of the home; and S is the lognormal shadow fading in dB. The shadow fading term, S, has an rms value of σ dB, and for each home PL_0 and γ are chosen such that σ is minimized.

2.2. *Scatter Plots*

Figure 3 shows the scatter plot of the path loss as a function of T-R separation for all homes. Equation (3) states that, on a logarithmic scale the path loss corresponds to a straight line with a slope γ. This straight line provides the median value of the random path loss. This amounts to fitting a least squares linear regression line through the scatter of measured path loss points in dB such that the root mean square deviation of path loss points about the regression line is minimized. Random shadowing effects of the channel occur at locations where the T-R separation is the same but have different levels of clutter in their propagation paths. This random variable usually has a normal distribution. Figure 4 shows the distribution of shadow fading random variable S in a typical home. The normal distribution regression line fit to the dB values confirms the log-normality of shadow fading in one typical home among the 23 homes we have measured, which has been accepted by many researchers (See [3]-[14].).

2.3. *Key Findings*

All models in the literature, find values for PL_0, γ, and σ that fit the global data population (i.e., the data from all homes pooled together.) in equation (3). Knowledge of PL_0, γ, and σ for propagation channel is useful only in a limited way as it averages the effect of indoor structure out of the data. A good model will predict propagation in homes where no measurements have been performed. In our experiments, we observed that these parameters did indeed change from one home to another and that taking measurements in one home alone would not fully represent the parameters in another home. This motivated us to assume that the propagation parameters PL_0, γ, and σ could be treated as random variables for each home and one can characterize their distribution by taking measurements in fewer homes than one. We found some interesting results.

In NLOS locations, the intercept point PL_0 depends on the materials blocking the signal within 1m of T-R separation and the home structure. The measured values of PL_0 for NLOS were very close to that of LOS path loss plus a few dB more loss due to the obstacle(s) blocking the LOS path. For ease of modeling, we excluded the frequency dependency of this parameter and set the intercept value to a fixed-value of 47 dB and 51 dB for LOS and NLOS, respectively for all homes. We then computed the least-square value of γ for each home. There was a very little change in γ and σ.

The values of γ change from one home to another and have a normal distribution N[$\mu_{\gamma},\sigma_{\gamma}$]. Figure 5 depicts the distribution of the path loss exponent, γ. The statistical values for PL_0, γ and σ are presented in Table I. These values were comparable with results found for wideband indoor channels in the literature with the exception of shadowing.

Over the population of our data, we note that shadow fading S is a zero mean Gaussian RV (See Figure 4.) with variance σ in dB that also varies from one home to another. The values of σ have normal distribution N[μ_S ,σ_S], whose mean μ_S and standard deviation σ_S are determined statistically from the measured data. Figure 6 illustrates the distribution of standard deviation of shadow fading σ in all homes.

The statistical values of the path loss model parameters are summarized in Table 1.

Table 1: Statistical values of the path loss model parameters.

	LOS		**NLOS**	
	Mean	**Std. Dev.**	**Mean**	**Std. Dev.**
PL_0 **(dB)**	47	NA	50.5	NA
γ	1.7	0.3	3.5	0.97
σ **(dB)**	1.6	0.5	2.7	0.98

3. The model

Base on the above observations, we have constructed a statistical path loss model for UWB propagation in indoor environments. The model is based on 300,000, 1.25 GHz wide UWB frequency responses taken at 5 GHz in 23 homes. In this section, we give detail description of the model.

Starting with equation (3), the path loss in dB as a function of distance is

$$PL(d) = PL_0 + 10 \cdot \gamma \log_{10}\left(\frac{d}{d_0}\right) + S(d);\ d \geq d_0 \quad (4)$$

PL_0, γ, and σ are characterized as follows.

The Intercept Point, PL_0: PL_0 is a fixed quantity and is given in Table 1, for LOS and NLOS environments.

The γ Parameter: The values of γ also change from one home to another and have a normal distribution N[$\mu_\gamma, \sigma_\gamma$]. That is

$$\gamma = \mu_\gamma + n_1\sigma_\gamma \quad (5)$$

Where n_1 is zero-mean Gaussian variate of unit standard deviation N[0,1].

The S Parameter: The shadow fading S varies randomly from one location to another location within any home. It is a zero-mean Gaussian variate with standard deviation σ which itself is a Gaussian variate over all homes. This can be represented mathematically as:

$$\begin{aligned} S &= n_2\sigma \\ \sigma &= \mu_\sigma + n_3\sigma_\sigma \end{aligned} \quad (6)$$

Where n_2 and n_3 are zero-mean Gaussian variate of unit standard deviation N[0,1].

By inserting (5) and (6) into (4), we get:

$$\overline{PL(d)}\Big|_{\text{dB}} = \left[PL_o + 10\left(\mu_\gamma + n_1\sigma_\gamma\right)\log_{10} d\right] + \left[n_2\left(\mu_\sigma + n_3\sigma_\sigma\right)\right] \quad (7)$$

After rearranging equation (7) we have:

$$\overline{PL(d)}\Big|_{\text{dB}} = \left[PL_o + 10\mu_\gamma \log_{10} d\right] + \left[10n_1\sigma_\gamma \log_{10} d + n_2\mu_\sigma + n_2n_3\sigma_\sigma\right];\quad 1\text{ m} \leq d \leq 20\text{ m} \quad (8)$$

The first bracketed term of equation (8) is the median path loss and the second bracketed term represents the random variation about the median path loss. The variable part of equation (8) is not exactly Gaussian due to the fact that $n_2 \times n_3$ is not Gaussian. However, this product is small with respect to the other two Gaussian terms. Therefore, it can be approximated as a zero mean random variate with standard deviation of:

$$\sigma_{\text{var}} = \sqrt{100\sigma_\gamma^2 \left(\log_{10} d\right)^2 + \mu_\sigma^2 + \sigma_\sigma^2} \qquad (9)$$

The distribution of σ_{var} is shown in Figure 8 on. The simulation results follow the Gaussian distribution closely, proving our intuition.

Finally, in using this model for simulations, it would be practical to use truncated Gaussian distributions for n_1, n_2 and n_3 so as to keep γ, and σ from taking on impractical values. One possibility is to confine them to the following ranges:

$$n_1 \in [-0.75, 0.75] \,\&\, n_2, n_3 \in [-2, 2]$$

Figure 7 illustrates the scatter plot of the simulated model versus measurements. It is readily seen that the model does closely follow the measured data.

4. Summary

We presented a statistical path loss model for indoor UWB signals of nominal center frequency of 5 GHz in indoor environments. The model is based on extensive propagation study in 23 homes. The model makes distinction between the main parameters of the propagation path loss from one home to another. The model has capability of even more refinement as more data becomes available.

5. References:

[1] K. Pahlavan, A.H. Levesque, *Wireless Information Networks*, John Wiley and Sons, New York, 1995.

[2] T.S. Rappaport, *Wireless Communications, Principles and Practice*, Prentice-Hall, New Jersey, 1996.

[3] A.A. Saleh, R.A. Valenzuela, "A Statistical Model For Indoor Multipath Propagation", *IEEE J. Select. Areas Commun.*, 5:128-137, Feb. 1987.

[4] R.J.C. Bultitude, S.A. Mahmoud, W.A. Sullivan, "A Comparison of indoor radio propagation characteristics at 910 MHz and 1.75 GHz", *IEEE J. Select. Areas Commun.*, 7:20-30, Jan 1989.

[5] T.S. Rappaport, S.Y. Seidel, K. Takamizawa, "Statistical Channel Impulse Response Models for Factory and Open Plan Building Radio Communication System Design", *IEEE Trans. on Commun.*, 39:794-806, May 1991.

[6] S.S. Ghassemzadeh, V. Erceg, D.L. Schilling, M. Taylor, H. Arshad, "Indoor Propagation and Fading Characterization of Spread Spectrum Signal at 2 GHz", *IEEE Globecom*, 92.

[7] S.S. Ghassemzadeh, D.L. Schilling, Z. Hadad, "On the Statistics of Multipath Fading Using a Direct Sequence CDMA signal at 2 GHz", *International Journal on Wireless Information Networks*, April 1994.

[8] V. Erceg, L. Greenstein, S. Tjandra, S. Parkoff, A. Gupta, B Kulic, A. Julius, R. Bianchi "An Empirically Based Path Loss Model for Wireless Channels in Suburban Environments", *IEEE J. Select. Areas Commun.*, 17:1205-1211, July 1999.

[9] S.J. Howard, K. Pahlavan, " Measurement and Analysis of the indoor radio channel in the frequency domain", *IEEE Trans. Instrum. Measure.*, 39:751-755, Oct. 1990.

[10] S.J. Howard, K. Pahlavan, "Autoregressive Modeling of Wide-Band Indoor Radio Propagation", *IEEE Transaction on Commun.*, 40:1540-1552, September 1992.

[11] H. Hashemi, "The indoor Propagation Channel", *Proc. of the IEEE*, 81:943-968, July, 1993

[12] M.Z. Win, R.A. Scholtz, M.A. Barnes, "Ultra-Wide Bandwidth Signal Propagation For Indoor Wireless Communications", *Proc. of IEEE Int. Conf. Commun*., 1:56-60, June 1997.

[13] D. Cassioli. A. Molisch, M.Z. Win, "A Statistical Model for UWB Indoor Channel", *Proc. of the IEEE VTC Spring 2001*, 2001 Rhodes.

[14] K. Siwiak, A. Petroff, "A Path Link Model for Ultra Wide Band Pulse Transmissions", *Proc. of the IEEE VTC Spring 2001*, 2001 Rhodes.

[15] R. Addler, D. Cheung, E. Green, M. Ho, Q. Li. C. Prettie, L. Rusch, K. Tinsley, "UWB Channel Measurements for the Home Environment", *UWB Intel Forum*, 2001 Oregon.

[16] S.S. Ghassemzadeh, et.al. "A Statistical Path Loss Model for In-Home UWB Channels", *Proc. of the IEEE Conference on UWB Systems and technologies*, May 2002 Baltimore.

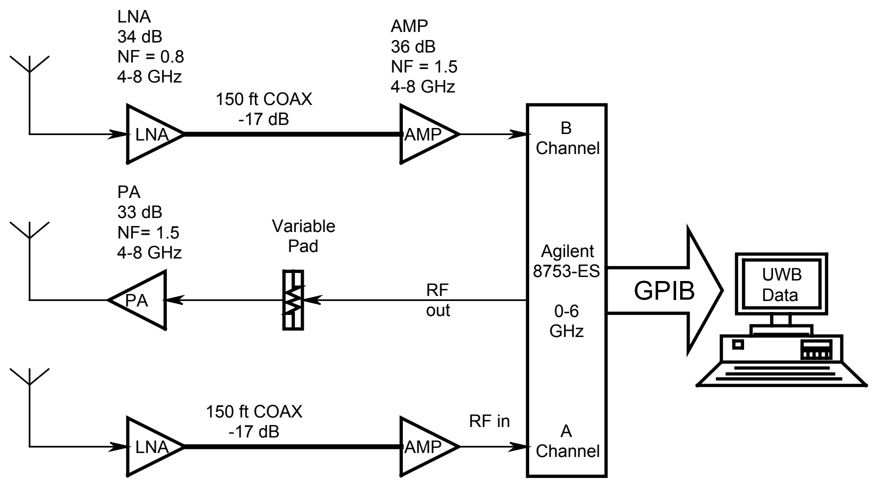

Figure 1: Channel Sounder Transceiver

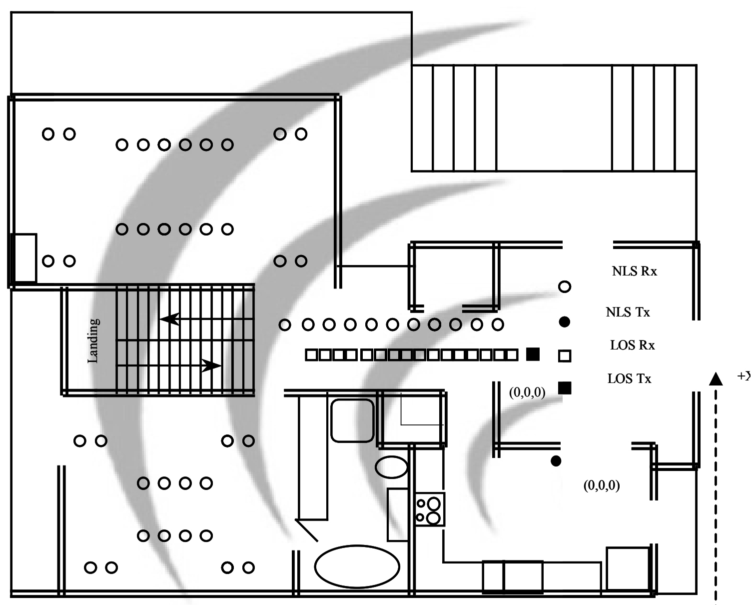

Figure 2: Typical home layout and experiment setup.

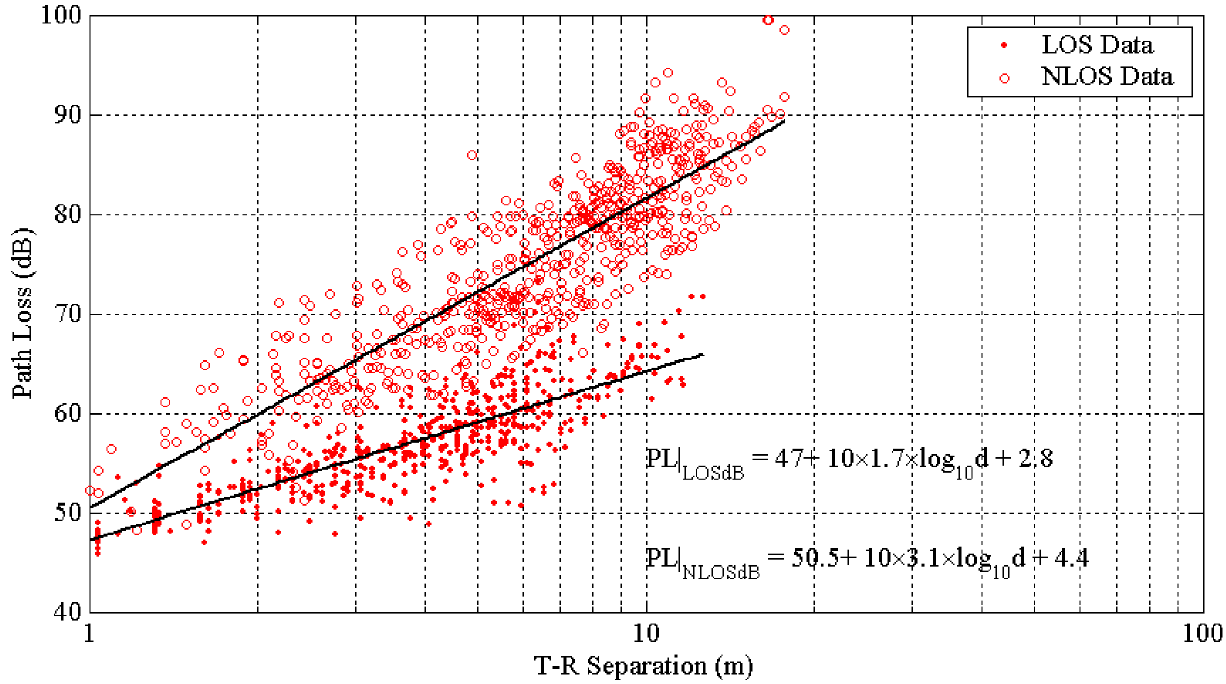

Figure 3: Scatter plot of decibel-path loss vs. decibel-distance in meters.

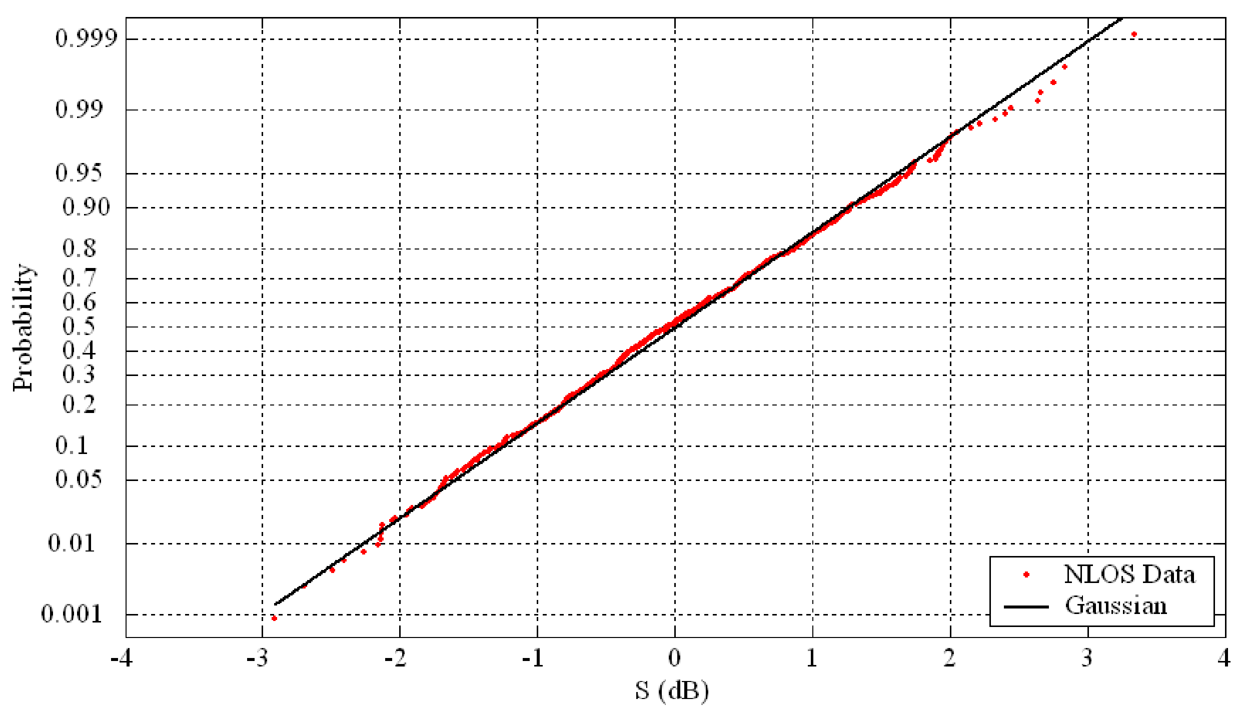

Figure 4: CDF of shadow fading in typical home, confirming Log-normal shadow fading.

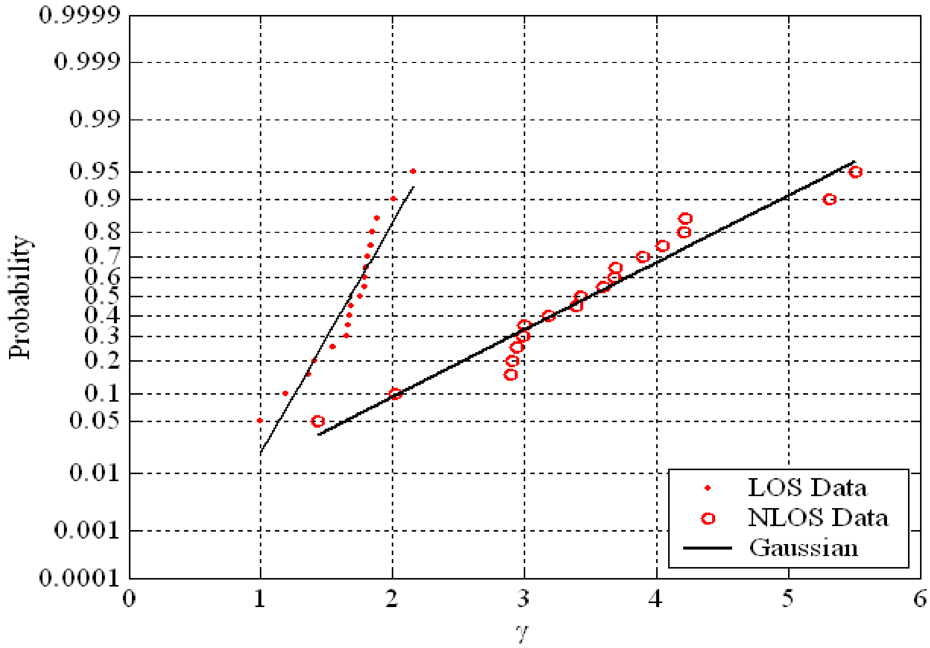

Figure 5: CDF of the path loss exponent.

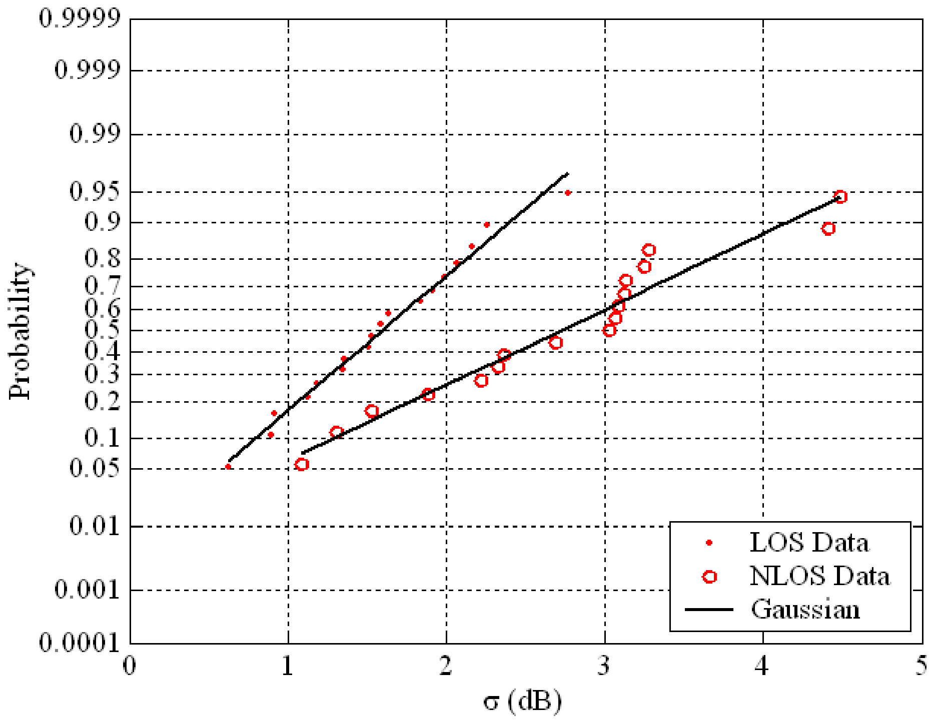

Figure 6: CDF of the standard deviation of shadow fading

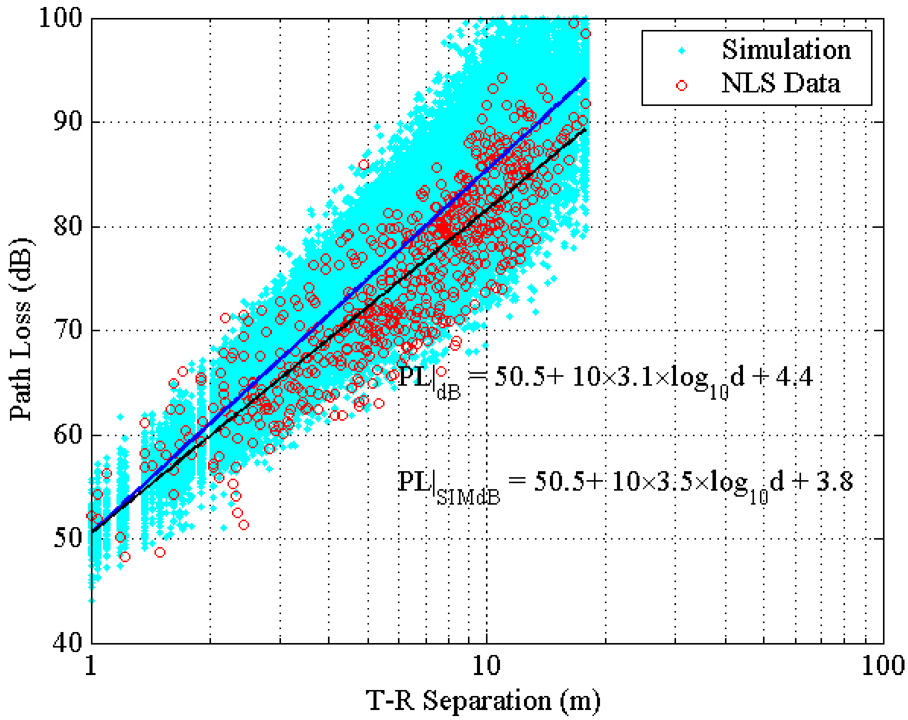

Figure 7: Model Simulation vs. Measurements.

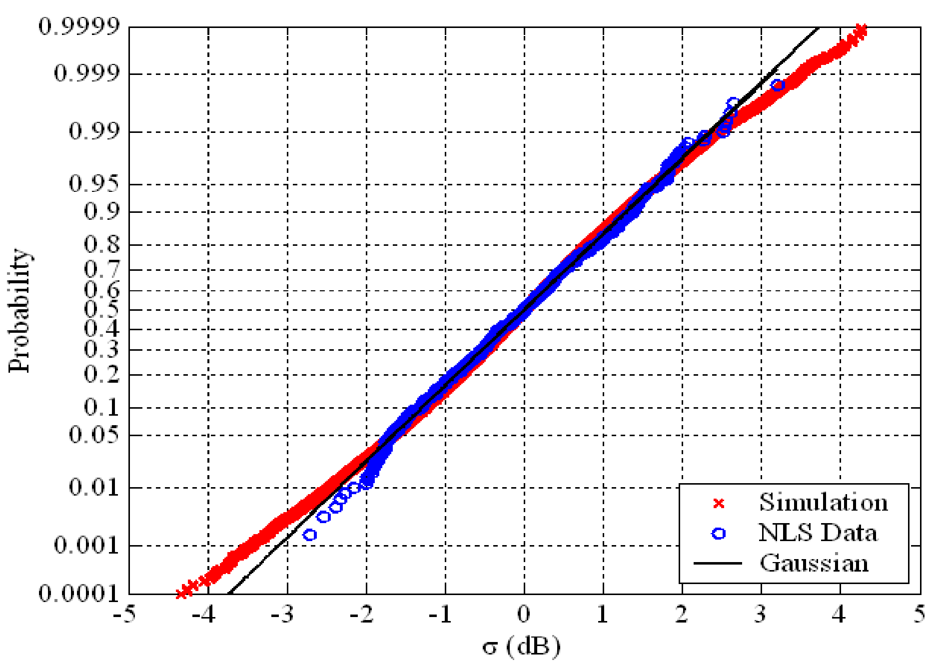

Figure 8: Standard deviation of the UWB path loss model.